Nanoscale Research Letters
a SpringerOpen Journal

NANO EXPRESS Open Access

In situ growth of $CuInS_2$ nanocrystals on nanoporous TiO_2 film for constructing inorganic/organic heterojunction solar cells

Zhigang Chen[1*], Minghua Tang[2], Linlin Song[1], Guoqiang Tang[1], Bingjie Zhang[1], Lisha Zhang[3], Jianmao Yang[1,4] and Junqing Hu[1]

Abstract

Inorganic/organic heterojunction solar cells (HSCs) have attracted increasing attention as a cost-effective alternative to conventional solar cells. This work presents an HSC by *in situ* growth of $CuInS_2$ (CIS) layer as the photoabsorption material on nanoporous TiO_2 film with the use of poly(3-hexylthiophene) (P3HT) as hole-transport material. The *in situ* growth of CIS nanocrystals has been realized by solvothermally treating nanoporous TiO_2 film in ethanol solution containing $InCl_3 \cdot 4H_2O$, $CuSO_4 \cdot 5H_2O$, and thioacetamide with a constant concentration ratio of 1:1:2. $InCl_3$ concentration plays a significant role in controlling the surface morphology of CIS layer. When $InCl_3$ concentration is 0.1 M, there is a layer of CIS flower-shaped superstructures on TiO_2 film, and CIS superstructures are in fact composed of ultrathin nanoplates as 'petals' with plenty of nanopores. In addition, the nanopores of TiO_2 film are filled by CIS nanocrystals, as confirmed using scanning electron microscopy image and by energy dispersive spectroscopy line scan analysis. Subsequently, HSC with a structure of FTO/TiO_2/CIS/P3HT/PEDOT:PSS/Au has been fabricated, and it yields a power conversion efficiency of 1.4%. Further improvement of the efficiency can be expected by the optimization of the morphology and thickness of CIS layer and the device structure.

Keywords: $CuInS_2$ film; *In situ* growth; TiO_2; P3HT; Heterojunction solar cells

PACS: 81.15.-z; 84.60.Jt; 73.40.Lq

Background

The quest and demand for clean and economical energy sources have increased interest in the development of various solar cells [1], such as Si solar cells [2], Cu(In, Ga)$(S,Se)_2$ film solar cells [3-6], organic solar cells [7], and dye-sensitized solar cells (DSSCs) [8-12]. Among these solar cells, DSSCs have been currently attracting widespread scientific and technological interest due to their low cost and high efficiency [8-12]. The typical working principle of DSSCs is based on ultrafast electron injection from a photoexcited dye into the conduction band of TiO_2 and subsequent dye regeneration and hole transportation to the counter electrode. The power conversion efficiency of DSSCs with organic solvent-based electrolyte has been reported to exceed 11% [9,13,14]. However, DSSCs still suffer from some problems, such as high cost of Ru-based dyes, leakage and/or evaporation from organic solvent-based electrolyte.

For reducing the cost, the use of inorganic semiconductor nanocrystals instead of Ru-based dyes in DSSCs has attracted an enormous interest [15-18]. Semiconductor nanocrystals as the sensitizers have many fascinating advantages, such as high extinction coefficients, large intrinsic dipole moments, and the tuned bandgap [19]. In particular, semiconductor quantum dots have capability of producing multiple electron/hole pairs with a single photon through the impact ionization effect [20]. For depositing semiconductor nanocrystals on TiO_2 films, two typical approaches have been developed. The first and most common route is the *in situ* synthesis of the nanocrystals on TiO_2 film, for example, by chemical bath deposition [21] or by successive ionic layer

* Correspondence: zgchen@dhu.edu.cn
[1]State Key Laboratory for Modification of Chemical Fibers and Polymer Materials, College of Materials Science and Engineering, Donghua University, Shanghai 201620, China
Full list of author information is available at the end of the article

adsorption and reaction (SILAR) [22]. This method provides high surface coverage, but the lack of capping agents leads to a broad size distribution and a higher density of surface defects of nanocrystals, which deteriorates solar cell performance [23]. The second route is the assembly of already-synthesized nanocrystals to TiO_2 substrates by direct adsorption [24] or linker-assisted adsorption [15]. This *ex situ* approach could achieve better control over the sizes and electronic properties of nanocrystals but suffers from low surface coverage and poor electronic coupling [23]. Up to now, many different semiconductor nanocrystals as the sensitizers have been investigated, including CdSe [17,22,25], CdS [21,26], and PbS [27-29]. Unfortunately, these metal chalcogenide semiconductors are easily oxidized when exposed to light, and this unfavorable situation is even more detrimental when the metal sulfide is in contact with a liquid electrolyte containing sulfur. It is well known that the choice of semiconductors and the method of their deposition play a paramount role in affecting cell efficiency. Therefore, it is still necessary to develop new materials and deposition methods for improving DSSCs with semiconductors as the sensitizers.

On the other hand, for avoiding the sealing problem in DSSCs, many attempts have been made to substitute liquid electrolytes with quasi-solid electrolytes [30] or solid-state hole transporting material (HTM) [31]. Similarly, when semiconductor nanocrystals are used as the sensitizers, some HTMs including poly(3-hexylthiophene) (P3HT) have been developed, resulting in the construction of all-solid-state inorganic/organic heterojunction solar cells (HSCs) [32-36], which possesses the advantages of both DSSCs and traditional organic solar cells. In particular, the efficiency of HSCs with the structure of TiO_2/Sb_2S_3/P3HT has reached 5% [32], which is very close to the efficiencies reported for solid DSSCs using Ru-based molecular dyes. In addition, Sb_2S_3 nanocrystals are nontoxic compared with Cd/Pb-based semiconductors. These facts show the great potentiality of all-solid HSCs, which also encourages to further achieve other kind of robust, efficient, and cheap HSCs without toxic component.

Copper indium disulfide ($CuInS_2$, abbreviated as CIS) has a small direct bandgap of 1.5 eV that matches well the solar spectrum, a large absorption coefficient ($\alpha = 5 \times 10^5\ cm^{-1}$), and low toxicity. It has been regarded to be a promising light-absorbing material for film solar cells [4]. As semiconductor sensitizers in DSSCs, CIS nanocrystals have been prepared by different methods and then were coated/adsorbed on TiO_2 film to construct DSSCs with liquid electrolyte [24,37,38]. In addition, the *in situ* growth of CIS on TiO_2 film has also been realized, by electrodeposition [16], spin-coating/anneal [39], and SILAR method [40], to construct DSSCs with liquid electrolyte. However, there is little report on solvothermal growth of CIS nanocrystals on TiO_2 film for the construction of all-solid HSCs. In this paper, we report a facile one-step solvothermal route for the *in situ* growth CIS nanocrystals on nanoporous TiO_2 film. The effects of reagent concentration on the surface morphology of CIS have been investigated. The all-solid HSC with the structure of FTO/compact-TiO_2 /nanoporous-TiO_2/CIS/P3HT/PEDOT:PSS/Au is fabricated, and it exhibits a relatively high conversion efficiency of 1.4%.

Methods

Materials

All of the chemicals were commercially available and were used without further purification. Titanium butoxide, petroleum ether, $TiCl_4$, $CuSO_4 \cdot 5H_2O$, $InCl_3 \cdot 4H_2O$, thioacetamide, ethanol, methanol, and 1,2-dichlorobenzene were purchased from Sinopharm Chemical Reagent Co., Ltd. (Shanghai, China). TiO_2 (P25) was obtained from Degussa. Transparent conductive glass (F:SnO_2, FTO) was purchased from Wuhan Geao Instruments Science & Technology Co., Ltd (Wuhan, Hubei, China). P3HT was bought from Guanghe Electronic Materials Co., Ltd. (Henan, China). The poly(3-4-ethylenedioxythiophene) doped with poly(4-stylenesulfonate) (PEDOT:PSS) solution (solvent, H_2O; weight percentage, 1.3%) was obtained from Aldrich (St. Louis, MO, USA).

Preparation of compact and nanoporous TiO_2 film

A part of FTO glass was chemically etched away in order to prevent direct contact between the two electrodes. A compact (about 100-nm thick) TiO_2 layer was first deposited onto the FTO glass as follow [41]. FTO glass was dipped into the mixture of titanium butoxide and petroleum ether (2:98 *V*/*V*), taken out carefully, hydrolyzed in air for 30 min, and sintered in oven for 30 min at 450°C.

Then, nanoporous TiO_2 films were prepared by the doctor-blading technique with TiO_2 (P25) colloidal dispersion and subsequently sintered at 450°C for 30 min, according to a previous study [42]. This film was soaked into a $TiCl_4$ (20 mM in water) solution for 12 h. It was then washed with deionized water and ethanol, dried with air, and sintered again at 450°C for 30 min.

In situ solvothermal growth of $CuInS_2$ nanocrystals

CIS layer was *in situ* grown on nanoporous TiO_2 films by a solvothermal process. In a typical process, thioacetamide (0.24 mmol, 0.02 M) was added into a 12 mL ethanol solution containing $InCl_3 \cdot 4H_2O$ (0.01 M) and $CuSO_4 \cdot 5H_2O$ (0.01 M) under magnetic stirring, until a clear solution was formed. The resulting solution was transferred into a Teflon-lined stainless steel autoclave with 30-mL capacity. Subsequently, FTO/compact-TiO_2/nanoporous-TiO_2 film as the substrate was vertically

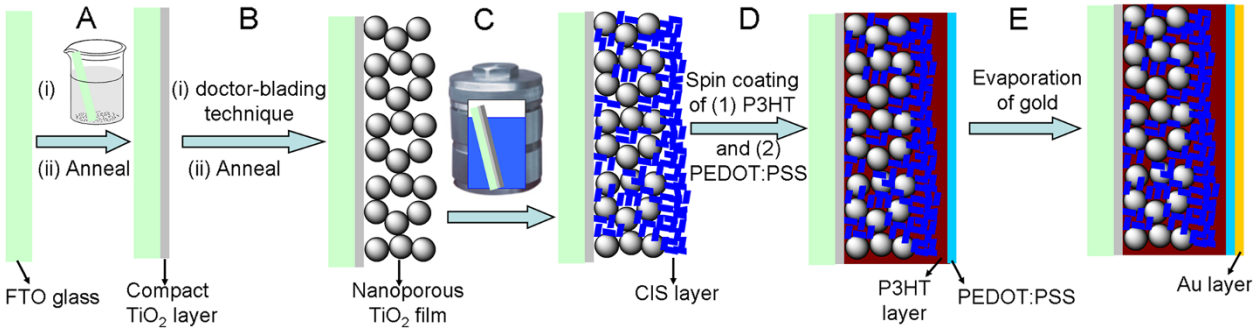

Figure 1 Schematic illustration of the fabrication process of FSCs. (A) preparation of compact TiO_2 film; **(B)** preparation of nanoporous TiO_2 film; **(C)** solvothermal growth of CIS layer; **(D)** spin-coating of P3HT and PEDOT:PSS; **(E)** evaporation of gold layer.

immersed into the solution. Lastly, the autoclave was kept in a fan-forced oven at 160°C for 12 h. After air-cooling to room temperature, CIS film on non-conductive glass side was scraped off, while CIS film on nanoporous TiO_2 film side was washed with deionized water and absolute ethanol successively, and dried in air. For comparison, the effects of $InCl_3 \cdot 4H_2O$ concentrations (0.01, 0.03, 0.1 M) on the morphologies CIS layer were investigated. The concentration ratio of $InCl_3 \cdot 4H_2O$, $CuSO_4 \cdot 5H_2O$, and thioacetamide was maintained constant (1:1:2) for all the cases.

Fabrication of all-solid HSC

The P3HT solution (10 mg/mL in 1,2-dichlorobenzene) was spin-coated onto TiO_2/CIS with 3,000 rpm for 60 s. Then, in order to improve the contact between P3HT and gold, a PEDOT:PSS solution diluted with two volumes of methanol was introduced onto TiO_2/CIS/P3HT layer by spin-coating at 2,000 rpm for 30 s [32]. In order to form a hybrid heterojunction, the TiO_2/CIS/P3HT/PEDOT:PSS layer was then annealed at 90°C for 30 min in a vacuum oven. Gold layer as the back contact was prepared by magnetron sputtering with a metal mask, giving an active area of 16 mm^2 for each device. The resulting HSC has a structure of FTO/compact-TiO_2/nanoporous-TiO_2/CIS/P3HT/PEDOT:PSS/Au.

Characterization and photoelectrical measurements

The sizes and morphologies of the sample were investigated by field emission scanning electron microscopy (FE-SEM; S-4800, Hitachi, Chiyoda-ku, Japan). During SEM measurement, energy dispersive spectroscopy (EDS; Quantax 400, Bruker AXS, Inc., Madison, WI, USA) line scan was also performed to locate and determine the distribution of different layer in the composite film. The X-ray diffraction (XRD; D/max-g B, Rigaku, Shibuya-ku, Japan) measurement was carried out using a Cu Kα radiation source ($\lambda = 1.5418$ Å). An ultraviolet/visible (UV-vis) spectrophotometer (U-3010 spectrophotometer, Hitachi, Chiyoda-ku, Japan) was used to carry out the optical measurements. The photocurrent density/voltage curves of HSC was measured under illumination (100 mW cm^{-2}) using a computerized Keithley Model 2400 Source Meter unit (Keithley Instruments Inc., Cleveland, OH, USA) and a 300-W xenon lamp (Newport 69911, Newport-Oriel Instruments, Stratford, CT, USA) serving as the light source.

Results and discussion

Herein, the fabrication of all-solid HSC with the structure of FTO/compact-TiO_2 /nanoporous-TiO_2/CIS/P3HT/PEDOT:PSS/Au involved five steps, as demonstrated in Figure 1. The first step was to prepare a compact TiO_2 layer by a dip-coating-anneal process (Figures 1 (step A) and 2), according our previous study [41]. SEM images (Figure 2) confirm the formation of a dense TiO_2 layer on FTO glass, and this TiO_2 layer has a thickness of about 300 nm. The presence of compact TiO_2 layer can not only improve the ohmic contact but also avoid short circuiting and/or loss of current by forming a blocking layer between FTO and P3HT in the HSC.

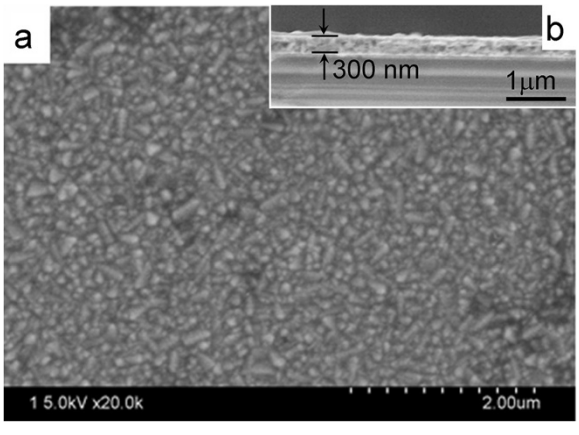

Figure 2 Surface (a) and cross-sectional (b) SEM images of dense TiO_2 layer.

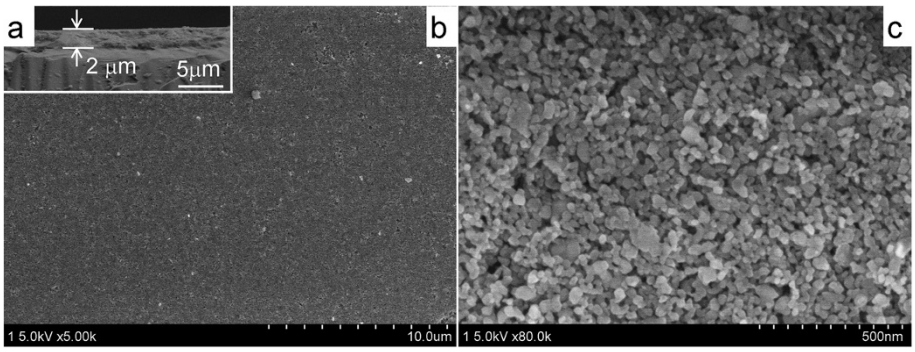

Figure 3 SEM images of nanoporous TiO_2 film: (a) cross-sectional, (b) low-, and (c) high-magnification SEM images of the surface.

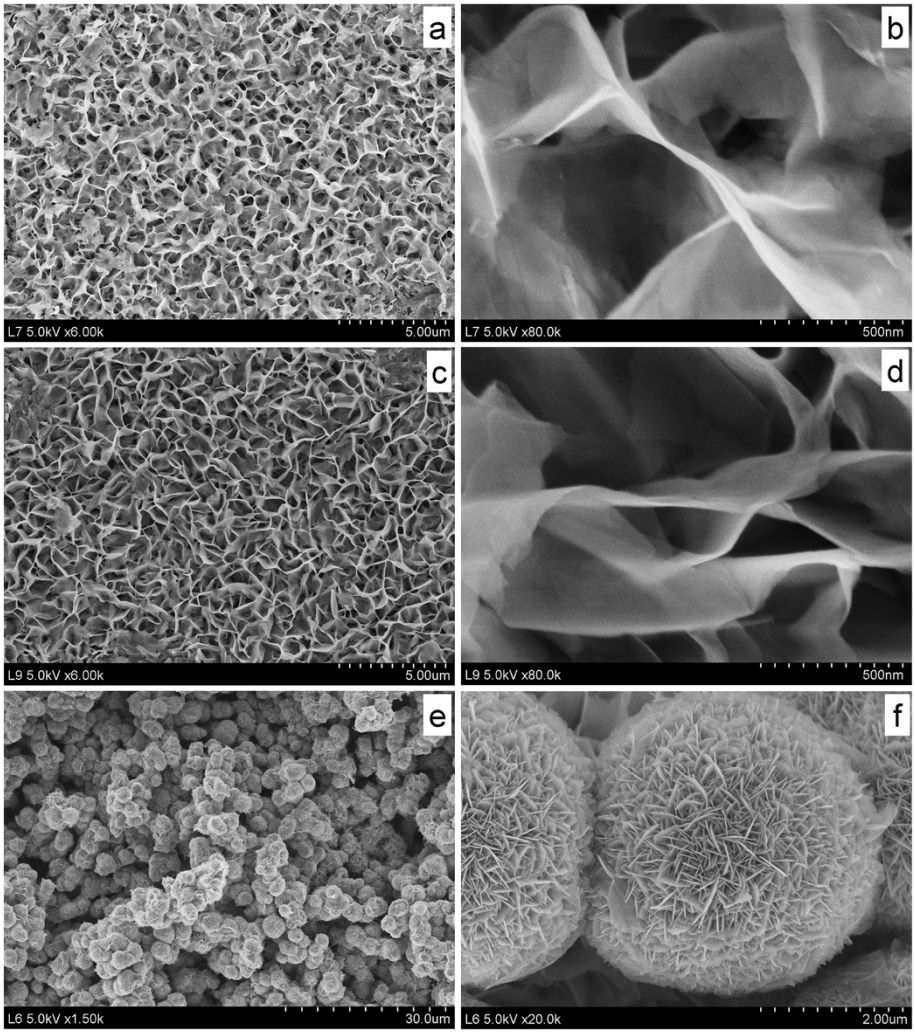

Figure 4 SEM images of CIS layer on TiO_2 film, obtained by a solvothermal treatment. At 160°C for 12 h with different $InCl_3$ concentration: **(a**,**b)** 0.01 M; **(c**,**d)** 0.03 M; **(e**,**f)** 0.1 M.

The second step was to fabricate nanoporous TiO_2 film on FTO/compact-TiO_2 by a classic doctor-blading -anneal technique with TiO_2 (P25) colloidal dispersion (Figures 1 (step B) and 3) [42]. Such nanoporous TiO_2 film has a thickness of about 2 μm, as revealed by cross-sectional SEM image (Figure 3a). In addition, one can find that the surface of nanoporous TiO_2 film is uniform and smooth without crack (Figure 3b). High-resolution SEM (Figure 3c) reveals the TiO_2 film to be composed of a three-dimensional network of interconnected particles with an average size of approximately 30 nm. It also can be found that there are many nanopores in the TiO_2 film, which facilitates to absorb dye and/or other semiconductor nanocrystals.

The third step was to *in situ* grow CIS nanocrystals on nanoporous TiO_2 film by the classic solvothermal process (Figure 1C), where FTO/compact-TiO_2/nanoporous-TiO_2 film as the substrate was vertically immersed into the ethanol solution containing $InCl_3$, $CuSO_4$, and thioacetamide with constant concentration ratio (1:1:2) as the reactant, and the solution was solvothermally treated at 160°C for 12 h. It has been found that reactant concentrations play a significant role in the controlled growth of CIS films in our previous study [4]. Thus, the effects of reactant concentration (such as $InCl_3$ concentration: 0.01, 0.03, 0.1 M) on the surface morphologies of CIS layer were investigated by SEM observation. Figure 4 gives the typical morphologies of CIS films prepared with different $InCl_3$ concentration. When $InCl_3$ concentration is low (0.01 or 0.03 M), a large amount of high-ordered potato chip-shaped CIS nanosheet arrays are densely packed and uniformly covered over the entire surface of FTO/compact-TiO_2/nanoporous-TiO_2 film (Figure 4a,c), which is similar to the *in situ* growth of CIS on Cu foil [4]. More detailed nanostructure about CIS film can be observed using high-magnification SEM images (Figure 4b,d), where individual CIS nanosheet displays a crooked shape with a thickness of approximately 10 nm and length of approximately 2 μm. These CIS potato chip-shaped nanosheets are assembled and intermeshed with each other, forming a continuous net-like flat film. It should be noted that CIS chips may be too big to separate efficiently electron/hole pairs in the application of HSCs. As $InCl_3$ concentration increased to 0.1 M, CIS flower-shaped superstructures with an average diameter of 3 μm spread over the whole FTO/compact-TiO_2/nanoporous-TiO_2 film (Figure 4e). In fact, as shown in the SEM image with higher magnification (Figure 4f), CIS superstructures are composed of ultrathin nanoplates as 'petals' with an average thickness of approximately 10 nm and length of approximately 0.6 μm. These 'petals' were aligned perpendicularly to the spherical surface with clearly oriented layers, pointing toward a common center. In addition, many hierarchical nanopores could be found among spherical superstructures and also among their 'petals,' which would improve the physicochemical properties.

Subsequently, TiO_2/CIS film samples were further characterized. To confirm the structure and composition of samples with CIS prepared with 0.03 or 0.1 M $InCl_3$, their cross-sectional morphologies were investigated. Obviously, a new layer can be found on the nanoporous TiO_2 film, and the pores in TiO_2 film have been partly filled with some nanoparticles (Figure 5a,b). Since CIS flower-shaped superstructure prepared from 0.1 M $InCl_3$ is composed of ultrathin nanoplates as 'petals' and should be more suitable for HSC, we further analyzed the microstructure and local atomic composition of this film sample. Figure 5c shows the high-magnification SEM image in the middle of the cross section. Obviously, there are two kinds of nanoparticles. One has the relatively large diameter of about 20 to 50 nm, and it should be TiO_2 nanoparticles, according to the SEM image (Figure 3c) of TiO_2 film substrate. The other has the relatively small diameter of about 10 nm, and it should be CIS nanoparticles which were filled into the pores of TiO_2 films. Furthermore, the red arrow on the SEM image shown in Figure 5b indicates the scanning path of an electron beam, and a clear presentation of the

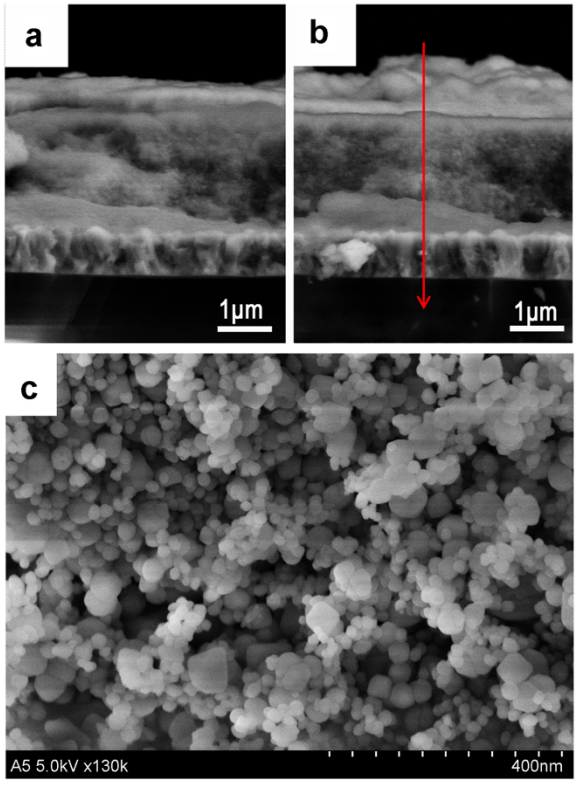

Figure 5 Cross-sectional SEM images of samples with CIS film prepared from (a) 0.03 M or (b,c) 0.1 M $InCl_3$.

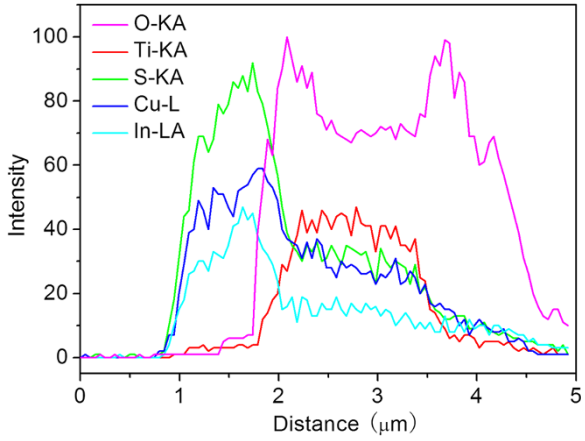

Figure 6 EDS line scan analysis along the red line indicated in the SEM image (Figure 5b).

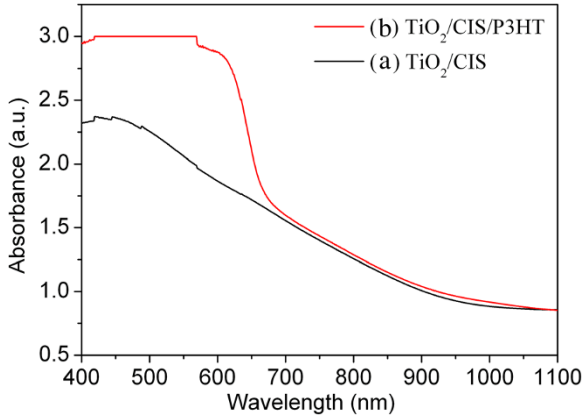

Figure 8 UV-vis/NIR absorption spectra. TiO_2/CIS **(a)** and TiO_2/CIS/P3HT **(b)** film samples.

elemental distribution is given by a plot of the EDS line scan signal versus the distance along the film (Figure 6). Overall, EDS line scan profile shows that the signal peaks of the Cu, In, and S elements locate at the first region, indicating the presence of CIS. Subsequently, all signals from Cu, In, and S elements exhibit an obvious drop and then a fairly flat upon further increase of scanning distance in the middle region. On the contrary, in this middle region, the signal from Ti and O elements increase rapidly and then exhibit a fairly flat upon further increase of scanning distance. The clear distinct difference in the spatial profiles from CIS and TiO_2 is well consistent with well-defined structures and SEM images, confirming that there is a CIS layer on the top of TiO_2 film, and the pores of TiO_2 film have been filled by CIS nanoparticles.

Furthermore, the phase and optical property of TiO_2/CIS film sample with CIS prepared with 0.1 M $InCl_3$ were investigated. Figure 7 shows the typical XRD pattern. Besides those existing peaks from SnO_2 (2θ: 26.6°, 33.8°, 37.8°, 51.7°, 61.8°, 65.8°; from FTO substrate) and TiO_2 film (2θ: 25.3°, 37.8°, 48.0°), the diffraction peaks at 27.8°, 46.5°, and 55.1° are assigned to (112), (204)/(220), and (312)/(116) planes of CIS, respectively, which are consistent with our previous study [4] and the data obtained from JCPDS card no. 85-1575. This fact confirms that CIS layer is well crystallized and has chalcopyrite structure. Furthermore, the optical absorption of TiO_2/CIS film was measured using a UV-vis spectrometer, as shown in Figure 8 (line A). This spectrum presents strong adsorption within a broad range between 400 and 800 nm, which is the characteristic absorption of CIS and consistent with our previous study [4].

The fourth step was to in turn deposit P3HT and PEDOT:PSS layer on FTO/compact-TiO_2/nanoporous-TiO_2/CIS film by the spin-coating process (Figure 1

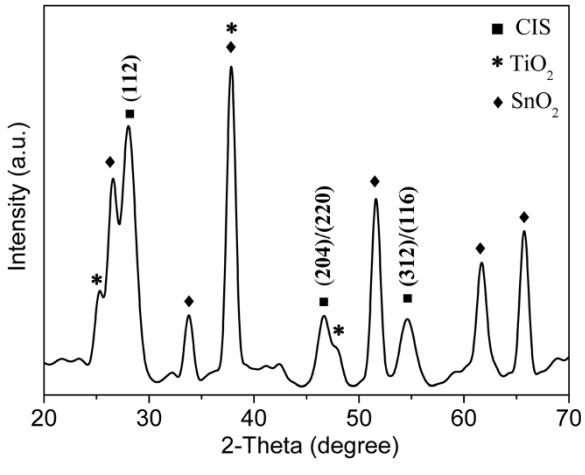

Figure 7 XRD pattern of TiO_2/CIS film sample, where CIS film was prepared from 0.1 M $InCl_3$.

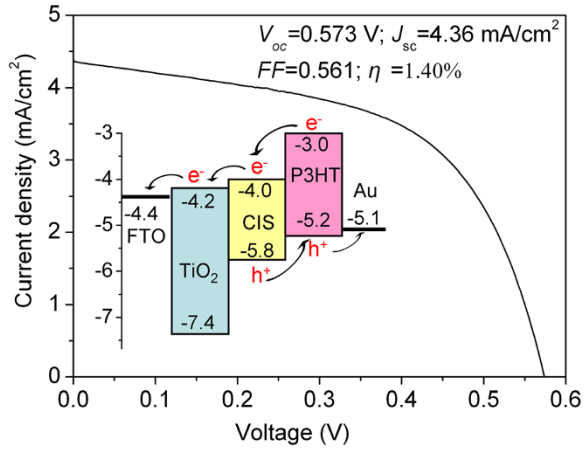

Figure 9 J-V characteristic curve of the HSC. The inset is band alignment among TiO_2, CIS, and P3HT.

(step D)). After the coating of P3HT, the photoabsorption of the film increases obviously in the range of 400 to 700 nm, as shown in Figure 8 (line B), since P3HT solution exhibits a wide and strong absorption with peak at about 445 nm [43]. This fact also indicates the efficient deposition of P3HT in/on TiO_2/CIS film. It should be noted that there are plenty of macro-pores among superstructures, nanopores inside CIS flower-shaped superstructures, and nanopores in TiO_2 film due to the insufficient filling. The hierarchical combination of smaller nanopores and larger macro-pores can be considered as transport paths [41]. It can be expected that P3HT solution can easily enter the deep layer of FTO/compact-TiO_2/nanoporous-TiO_2/CIS film through the transport paths, when they are coated onto its surface during the spin-coating process. This should lead to better effects of wetting and pore-filling and thus better interfacial contact among P3HT, CIS, and TiO_2, probably resulting in more efficient separation of photoinduced electron/hole pairs and thus higher photocurrent.

The last step was to prepare gold electrode with the thickness of 100 nm on the resulting film for completing the construction of HSC (Figure 1 (step E)). Photocurrent density/voltage characteristics of the resulted HSC are shown in Figure 9. The cell exhibits an open circuit voltage (V_{oc}) of 0.573 V, a short-circuit current density (J_{sc}) of 4.36 mA/cm^2, and a fill factor (*FF*) of 0.561, yielding an overall energy conversion efficiency (η) of 1.40%. This conversion efficiency has been greatly improved, compared with that (typically 0.1% to 1.0%) of TiO_2/P3HT hybrid HSCs in the absence of dye or PCBM [44-47]. There are chiefly three reasons for the improvement. The first reason is the good band alignment among TiO_2, CIS, and P3HT (the inset of Figure 9), resulting in the fact that exciton dissociation and charge transfer at the interface are energetically favorable. The second reason should be attributed to the strong photoabsorption of CIS and P3HT, as revealed in Figure 8, since the successful sensitization of TiO_2 by CIS layer has been well demonstrated by the previous studies [24,38,40]. The last reason results from the good interfacial contact among P3HT, CIS, and TiO_2 due to hierarchical pores in CIS and TiO_2 layer, as demonstrated in Figures 4 and 5. In addition, it should be noted that our cell efficiency (1.4%) is relatively low compared with that (3% to 5%) of HSC with the structure of TiO_2/Sb_2S_3/P3HT [32,36,48,49], which probably results from the large size of CIS, unoptimized cell structure, etc. Therefore, further improvement of the efficiency could be expected by the optimization of the morphology and thickness of CIS layer and the device structure.

Conclusions

In summary, an *in situ* growth of CIS nanocrystals has been demonstrated by solvothermally treating nanoporous TiO_2 film in ethanol solution containing $InCl_3 \cdot 4H_2O$, $CuSO_4 \cdot 5H_2O$, and thioacetamide with a constant concentration ratio of 1:1:2. When $InCl_3$ concentration is 0.1 M, there is a CIS layer on the top of TiO_2 film, and the pores of TiO_2 film have been filled by CIS nanoparticles. An HSC with the structure of FTO/TiO_2/CIS/P3HT/PEDOT:PSS/Au has been fabricated, and it yields a power conversion efficiency of 1.4%. Further improvement can be expected by optimizing CIS layer and the cell structure.

Competing interests

The authors declare that they have no competing interests.

Authors' contributions

ZC designed the experiment and wrote the article. ZC, MT, and LS carried out the laboratory experiments. GT, BZ, LZ, JY, and JH assisted the technical support for measurements (SEM, EDS, XRD, UV–vis/NIR absorption, and I-V) as well as the data analysis. All authors read and approved the final manuscript.

Acknowledgments

This work was financially supported by the National Natural Science Foundation of China (grant nos. 21107013, 21171035, and 51272299), Specialized Research Fund for the Doctoral Program of Higher Education (grant no. 20110075120012), the Scientific Research Foundation for the Returned Overseas Chinese Scholars, projects of the Shanghai Committee of Science and Technology (grant nos. 10JC1400100, 13JC1400300), Innovation Program of Shanghai Municipal Education Commission (grant no. 13ZZ053), the Fundamental Research Funds for the Central Universities, the Shanghai Leading Academic Discipline Project (grant no. B603), and the Program of Introducing Talents of Discipline to Universities (grant no. 111-2-04).

Author details

[1]State Key Laboratory for Modification of Chemical Fibers and Polymer Materials, College of Materials Science and Engineering, Donghua University, Shanghai 201620, China. [2]Analysis and Testing Center, Soochow University, Suzhou 215123, China. [3]College of Environmental Science and Engineering, Donghua University, Shanghai 201620, China. [4]Research Center for Analysis and Measurement, Donghua University, Shanghai 201620, China.

Received: 17 June 2013 Accepted: 8 August 2013
Published: 16 August 2013

References

1. Gratzel M: **Photoelectrochemical cells.** *Nature* 2001, **414:**338–344.
2. Peng KQ, Wang X, Li L, Wu XL, Lee ST: **High-performance silicon nanohole solar cells.** *J Am Chem Soc* 2010, **132:**6872–6873.
3. Jackson P, Hariskos D, Lotter E, Paetel S, Wuerz R, Menner R, Wischmann W, Powalla M: **New world record efficiency for Cu (In, Ga)Se_2 thin-film solar cells beyond 20%.** *Prog Photovolt Res Appl* 2011, **19:**894–897.
4. Tang M, Tian Q, Hu X, Peng Y, Xue Y, Chen Z, Yang J, Xu X, Hu J: ***In situ*** **preparation of $CuInS_2$ films on a flexible copper foil and their application in thin film solar cells.** *Cryst Eng Comm* 2012, **14:**1825–1832.
5. Zhang L, Song L, Tian Q, Kuang X, Hu J, Liu J, Yang J, Chen Z: **Flexible fiber-shaped $CuInSe_2$ solar cells with single-wire-structure: design, construction and performance.** *Nano Energy* 2012, **1:**769–776.
6. Reddy VR, Wu J, Manasreh MO: **Colloidal Cu(In_xGa_{1-x})Se_2 nanocrystals for all-inorganic nano-heterojunction solar cells.** *Mater Lett* 2013, **92:**296–299.
7. Lee K, Kim JY, Coates NE, Moses D, Nguyen TQ, Dante M, Heeger AJ: **Efficient tandem polymer solar cells fabricated by all-solution processing.** *Science* 2007, **317:**222–225.
8. Oregan B, Gratzel M: **A low-cost, high-efficiency solar-cell based on dye-sensitized colloidal TiO_2 films.** *Nature* 1991, **353:**737–740.
9. Gratzel M: **Conversion of sunlight to electric power by nanocrystalline dye-sensitized solar cells.** *J Photoch Photobio A* 2004, **164:**3–14.
10. Chen ZG, Li FY, Huang CH: **Organic d-pi-a dyes for dye-sensitized solar cell.** *Curr Org Chem* 2007, **11:**1241–1258.
11. Chen ZG, Li FY, Yang H, Yi T, Huang CH: **A thermostable and long-term-stable ionic-liquid-based gel electrolyte for efficient dye-sensitized solar cells.** *Chem Phys Chem* 2007, **8:**1293–1297.

12. Hagfeldt A, Boschloo G, Sun L, Kloo L, Pettersson H: **Dye-sensitized solar cells.** *Chem Rev* 2010, **110:**6595–6663.
13. Chen C-Y, Wang M, Li J-Y, Pootrakulchote N, Alibabaei L, C-h N-l, Decoppet J-D, Tsai J-H, Graetzel C, Wu C-G, Zakeeruddin SM, Grätzel M: **Highly efficient light-harvesting ruthenium sensitizer for thin-film dye-sensitized solar cells.** *ACS Nano* 2009, **3:**3103–3109.
14. Yella A, Lee H-W, Tsao HN, Yi C, Chandiran AK, Nazeeruddin MK, Diau EW-G, Yeh C-Y, Zakeeruddin SM, Graetzel M: **Porphyrin-sensitized solar cells with cobalt (II/III)-based redox electrolyte exceed 12 percent efficiency.** *Science* 2011, **334:**629–634.
15. Robel I, Subramanian V, Kuno M, Kamat PV: **Quantum dot solar cells. Harvesting light energy with CdSe nanocrystals molecularly linked to mesoscopic TiO_2 films.** *J Am Chem Soc* 2006, **128:**2385–2393.
16. Yun JH, Ng YH, Huang SJ, Conibeer G, Amal R: **Wrapping the walls of n-TiO_2 nanotubes with p-$CuInS_2$ nanoparticles using pulsed-electrodeposition for improved heterojunction photoelectrodes.** *Chem Commun* 2011, **47:**11288–11290.
17. Choi H, Santra PK, Kamat PV: **Synchronized energy and electron transfer processes in covalently linked CdSe-squaraine dye-TiO light harvesting assembly.** *ACS Nano* 2012, **6:**5718–5726.
18. Santra PK, Kamat PV: **Tandem-layered quantum dot solar cells: tuning the photovoltaic response with luminescent ternary cadmium chalcogenides.** *J Am Chem Soc* 2013, **135:**877–885.
19. Alivisatos AP: **Semiconductor clusters, nanocrystals, and quantum dots.** *Science* 1996, **271:**933–937.
20. Nozik AJ: **Exciton multiplication and relaxation dynamics in quantum dots: applications to ultrahigh-efficiency solar photon conversion.** *Inorg Chem* 2005, **44:**6893–6899.
21. Yan KY, Chen W, Yang SH: **Significantly enhanced open circuit voltage and fill factor of quantum dot sensitized solar cells by linker seeding chemical bath deposition.** *J Phys Chem C* 2013, **117:**92–99.
22. Lee H, Wang MK, Chen P, Gamelin DR, Zakeeruddin SM, Gratzel M, Nazeeruddin MK: **Efficient CdSe quantum dot-sensitized solar cells prepared by an improved successive ionic layer adsorption and reaction process.** *Nano Lett* 2009, **9:**4221–4227.
23. Mora-Sero I, Gimenez S, Fabregat-Santiago F, Gomez R, Shen Q, Toyoda T, Bisquert J: **Recombination in quantum dot sensitized solar cells.** *Accounts Chem Res* 2009, **42:**1848–1857.
24. Li TL, Teng HS: **Solution synthesis of high-quality $CuInS_2$ quantum dots as sensitizers for TiO_2 photoelectrodes.** *J Mater Chem* 2010, **20:**3656–3664.
25. Yu Y, Kamat PV, Kuno M: **A CdSe nanowire/quantum dot hybrid architecture for improving solar cell performance.** *Adv Funct Mater* 2010, **20:**1464–1472.
26. Chen C, Ali G, Yoo SH, Kum JM, Cho SO: **Improved conversion efficiency of CdS quantum dot-sensitized TiO_2 nanotube-arrays using $CuInS_2$ as a co-sensitizer and an energy barrier layer.** *J Mater Chem* 2011, **21:**16430–16435.
27. Etgar L, Park J, Barolo C, Nazeeruddin MK, Viscardi G, Graetzel M: **Design and development of novel linker for PbS quantum dots/TiO_2 mesoscopic solar cell.** *ACS Appl Mater Inter* 2011, **3:**3264–3267.
28. Benehkohal NP, Gonzalez-Pedro V, Boix PP, Chavhan S, Tena-Zaera R, Demopoulos GP, Mora-Sero I: **Colloidal PbS and PbSeS quantum dot sensitized solar cells prepared by electrophoretic deposition.** *J Phys Chem C* 2012, **116:**16391–16397.
29. Etgar L, Moehl T, Gabriel S, Hickey SG, Eychmueller A, Graetzel M: **Light energy conversion by mesoscopic PbS quantum dots/TiO_2 heterojunction solar cells.** *ACS Nano* 2012, **6:**3092–3099.
30. Chen ZG, Yang H, Li XH, Li FY, Yi T, Huang CH: **Thermostable succinonitrile-based gel electrolyte for efficient, long-life dye-sensitized solar cells.** *J Mater Chem* 2007, **17:**1602–1607.
31. Bach U, Lupo D, Comte P, Moser JE, Weissortel F, Salbeck J, Spreitzer H, Gratzel M: **Solid-state dye-sensitized mesoporous TiO_2 solar cells with high photon-to-electron conversion efficiencies.** *Nature* 1998, **395:**583–585.
32. Chang JA, Rhee JH, Im SH, Lee YH, Kim H-J, Seok SI, Nazeeruddin MK, Gratzel M: **High-performance nanostructured inorganic–organic heterojunction solar cells.** *Nano Lett* 2010, **10:**2609–2612.
33. Balis N, Dracopoulos V, Stathatos E, Boukos N, Lianos P: **A solid-state hybrid solar cell made of nc-TiO_2, CdS quantum dots, and P3HT with 2-amino-1-methylbenzimidazole as an interface modifier.** *J Phys Chem C* 2011, **115:**10911–10916.
34. Qian J, Liu Q-S, Li G, Jiang K-J, Yang L-M, Song Y: **P3HT as hole transport material and assistant light absorber in CdS quantum dots-sensitized solid-state solar cells.** *Chem Commun* 2011, **47:**6461–6463.
35. Liu CP, Wang HE, Ng TW, Chen ZH, Zhang WF, Yan C, Tang YB, Bello I, Martinu L, Zhang WJ, Jha SK: **Hybrid photovoltaic cells based on ZnO/Sb_2S_3/P3HT heterojunctions.** *Phys Status Solidi B* 2012, **249:**627–633.
36. Heo JH, Im SH, Kim H-J, Boix PP, Lee SJ, Seok SI, Mora-Sero I, Bisquert J: **Sb_2S_3-sensitized photoelectrochemical cells: open circuit voltage enhancement through the introduction of poly-3-hexylthiophene interlayer.** *J Phys Chem C* 2012, **116:**20717–20721.
37. Li TL, Lee YL, Teng H: **High-performance quantum dot-sensitized solar cells based on sensitization with $CuInS_2$ quantum dots/CdS heterostructure.** *Energ Environ Sci* 2012, **5:**5315–5324.
38. Santra PK, Nair PV, Thomas KG, Kamat PV: **$CuInS_2$-sensitized quantum dot solar cell. Electrophoretic deposition, excited-state dynamics, and photovoltaic performance.** *J Phys Chem Lett* 2013, **4:**722–729.
39. Zhou ZJ, Fan JQ, Wang X, Sun WZ, Zhou WH, Du ZL, Wu SX: **Solution fabrication and photoelectrical properties of $CuInS_2$ nanocrystals on TiO_2 nanorod array.** *ACS Appl Mater Inter* 2011, **3:**2189–2194.
40. Zhou ZJ, Yuan SJ, Fan JQ, Hou ZL, Zhou WH, Du ZL, Wu SX: **$CuInS_2$ quantum dot-sensitized TiO_2 nanorod array photoelectrodes: synthesis and performance optimization.** *Nanoscale Res Lett* 2012, **7:**652.
41. Chen ZG, Tang YW, Yang H, Xia YY, Li FY, Yi T, Huang CH: **Nanocrystalline TiO_2 film with textural channels: exhibiting enhanced performance in quasi-solid/solid-state dye-sensitized solar cells.** *J Power Sources* 2007, **171:**990–998.
42. Nazeeruddin MK, Kay A, Rodicio I, Humphrybaker R, Muller E, Liska P, Vlachopoulos N, Gratzel M: **Conversion of light to electricity by cis-x2bis (2,2′-bipyridyl-4,4′-dicarboxylate)ruthenium(ii) charge-transfer sensitizers (x = cl-, br-, i-, cn-, and scn-) on nanocrystalline TiO_2 electrodes.** *J Am Chem Soc* 1993, **115:**6382–6390.
43. Peng Y, Song G, Hu X, He G, Chen Z, Xu X, Hu J: ***In situ* synthesis of P3HT-capped CdSe superstructures and their application in solar cells.** *Nanoscale Res Lett* 2013, **8:**106.
44. Chuang C-H, Lin Y-Y, Tseng Y-H, Chu T-H, Lin C-C, Su W-F, Chen C-W: **Nanoscale morphology control of polymer/TiO_2 nanocrystal hybrids: photophysics, charge generation, charge transport, and photovoltaic properties.** *J Phys Chem C* 2010, **114:**18717–18724.
45. Gerein NJ, Fleischauer MD, Brett MJ: **Effect of TiO_2 film porosity and thermal processing on TiO_2-P3HT hybrid materials and photovoltaic device performance.** *Sol Energ Mat Sol Cells* 2010, **94:**2343–2350.
46. Zeng T-W, Ho C-C, Tu Y-C, Tu G-Y, Wang L-Y, Su W-F: **Correlating interface heterostructure, charge recombination, and device efficiency of poly(3-hexyl thiophene)/TiO_2 nanorod solar cell.** *Langmuir* 2011, **27:**15255–15260.
47. Tu Y-C, Lin J-F, Lin W-C, Liu C-P, Shyue J-J, Su W-F: **Improving the electron mobility of TiO_2 nanorods for enhanced efficiency of a polymer-nanoparticle solar cell.** *Cryst Eng Comm* 2012, **14:**4772–4776.
48. Im SH, Kim HJ, Rhee JH, Lim CS, Sang SI: **Performance improvement of Sb_2S_3-sensitized solar cell by introducing hole buffer layer in cobalt complex electrolyte.** *Energ Environ Sci* 2011, **4:**2799–2802.
49. Cardoso JC, Grimes CA, Feng XJ, Zhang XY, Komarneni S, Zanoni MVB, Bao NZ: **Fabrication of coaxial TiO_2/Sb_2S_3 nanowire hybrids for efficient nanostructured organic-inorganic thin film photovoltaics.** *Chem Commun* 2012, **48:**2818–2820.

doi:10.1186/1556-276X-8-354
Cite this article as: Chen *et al.*: ***In situ*** growth of $CuInS_2$ nanocrystals on nanoporous TiO_2 film for constructing inorganic/organic heterojunction solar cells. *Nanoscale Research Letters* 2013 **8**:354.